Optical Engineering

OpticalEngineering.SPIEDigitalLibrary.org

Optimized initial weight in quantum-inspired neural network for compressing computer-generated holograms

Shenhua Hou
Guanglin Yang
Haiyan Xie

SPIE.

Shenhua Hou, Guanglin Yang, Haiyan Xie, "Optimized initial weight in quantum-inspired neural network for compressing computer-generated holograms," *Opt. Eng.* **58**(5), 053105 (2019), doi: 10.1117/1.OE.58.5.053105.

Optimized initial weight in quantum-inspired neural network for compressing computer-generated holograms

Shenhua Hou,[a] Guanglin Yang,[a,*] and Haiyan Xie[b]
[a]Peking University, School of Electronic Engineering and Computer Science, Laboratory of Signal and Information Processing, Department of Electronics, Beijing, China
[b]China Science Patent Trademark Agents Ltd., Beijing, China

Abstract. We propose an optimized initial weight scheme in a quantum-inspired neural network for compressing computer-generated holograms (CGHs). An optimized initial weight generation strategy is applied to accelerate the compression process. The pixel blocks' complexity distribution of CGH is analyzed, and the parallel quantum neural network structure is used to compress the image pixel blocks. A deep convolutional neural network with residual learning is also adopted for improving the quality of the reconstructed image. The experimental results have shown that the compression iterations are reduced by using the optimized initial weight, and the reconstructed image quality of the compressed CGH is improved using the parallel quantum-inspired neural network structure and the deep convolutional neural network with residual learning. [DOI: 10.1117/1.OE.58.5.053105]

Keywords: computer-generated hologram; image processing; image reconstruction techniques; quantum optics; quantum information and processing.

Paper 190037 received Jan. 10, 2019; accepted for publication Apr. 30, 2019; published online May 24, 2019.

1 Introduction

In computer holography, a computer-generated hologram (CGH) contains a large quantity of information, including amplitude and phase information of an object, which requires much space for storage and bandwidth for transmission.[1] Therefore, it is necessary to reduce holographic data, while guaranteeing the reconstructed image quality of the processed CGH with a suitable and effective compression method.

Several works reporting on CGH compression have been proposed recently. In Ref. 2, a compression and transmission system for CGH with the low complexity lossless compression algorithm (LOCO-I) was provided, which proved that the CGH can be well reconstructed with lossy compression. Compressive sensing was also used to compress and transmit a CGH.[3] In this method, a CGH was subsampled using variable density sampling scheme and reconstituted using the subsampled data by Fourier transform and total variation minimization. However, the subsampling process cannot ensure that the key components for decompression were well selected and reserved. The conventional artificial neural network (ANN), which was widely adopted in nonlinear problems, also proved to be effective for CGH compression.[4,5] Because the CGH was an interference fringe pattern with nonlinear intensity distribution,[6] the ANN was suitable for intelligently processing the nonlinear hologram distribution. However, the ANN process was time-consuming and the memory capacity was limited.

A backpropagating quantum-inspired neural network (QINN) constructed from a quantum bit (qubit) neuron model has shown high efficiency in ordinary image compression applications.[7,8] It has shown that the better performance of qubit-based QINN is not simply due to the complex-valued neuron parameters but rather due to quantum superposition and its associated probability interpretation.[9] Inspired by this, the qubit-based QINN has been adopted in CGH compression in Ref. 1. The qubit-based QINN can accelerate CGH transmission speed as well as improve the image quality of the reconstructed CGH.

Despite the improvement using qubit-based QINN, the weight initialization of the qubit-based QINN can significantly affect the convergence speed and network generalization.[10] When the initial weight of the network is close to the optimal solution, the network only needs to be trained for a few iterations to reach a stable state. However, when the initial weight is far from the optimal solution, the network must be trained for an extended period of time. In the absence of efficient initialization, the qubit-based QINN for CGH compression still requires many iterations to converge. In addition, the image quality of the reconstructed CGH after network compression cannot be satisfied especially at high compression ratio (CR) and can be further improved.

In this paper, the QINN with an optimized initial weight is proposed to compress a CGH, as shown in Fig. 1. We first make use of a pretrained model generated from the CGH training set to initialize our qubit-based QINN, which can significantly reduce the compression time. Then we prove that the parallel structure can be an alternative strategy to improve the CGH compression performance. Moreover, we add a deep convolutional neural network (CNN) after compression to post-process and restore CGH. Our main contributions are summarized as follows: (i) an initialization strategy is applied to accelerate the transmission process of CGH and (ii) the applicability of the parallel qubit-based QINN structure and a deep CNN are analyzed, yielding better image quality of the reconstructed CGH.

2 Computer-Generated Hologram Principles

According to the principle of Leith and Upatnieks[11] in off-axis reference beam holograms, the amplitude and phase

*Address all correspondence to Guanglin Yang, E-mail: ygl@pku.edu.cn

0091-3286/2019/$25.00 © 2019 SPIE

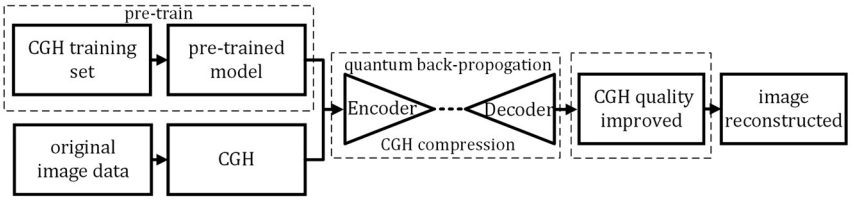

Fig. 1 CGH compression using a qubit-based QINN.

Table 1 Experimental parameters for a CGH.

Parameters	Value
Wavelength	633 nm
Original image size	128×128 pixels
Pixel size	0.00345×0.00345 mm
Hologram size	256×256 pixels

transmittance of a hologram $I(x,y)$ recorded under ideal conditions are as follows:

$$\begin{aligned} I(x,y) &= [r(x,y)+a(x,y)][r(x,y)+a(x,y)]^* \\ &= |R(x,y)\exp[j\phi(x,y)] + A(x,y)\exp[j\psi(x,y)]|^2 \\ &= R(x,y)^2 + A(x,y)^2 + 2R(x,y)A(x,y) \\ &\quad \cdot \cos[\phi(x,y) - \psi(x,y)], \end{aligned} \tag{1}$$

where the $r(x,y) = R(x,y)\exp[j\phi(x,y)]$ with amplitude $R(x,y)$ and phase $\phi(x,y)$ represents the titled reference wave and the $a(x,y) = A(x,y)\exp[j\psi(x,y)]$ with amplitude $A(x,y)$ and phase $\psi(x,y)$ represents the object wave. A CGH generated using Eq. (1) and parameters in Table 1 are showed in Fig. 2.

3 Quantum-Inspired Neural Network Compression for Computer-Generated Holograms

3.1 *Quantum Neuron Model*

According to the principles described in Ref. 7, a qubit state $|\psi\rangle$ which maintains a coherent superposition of $|1\rangle$ and $|0\rangle$ can be expressed as

$$|\psi\rangle = \alpha|0\rangle + \beta|1\rangle, \tag{2}$$

where α and β are the complex probability amplitudes. In addition, the quantum state can also be expressed conveniently by a complex number

$$f(\theta) = \cos\theta + i\sin\theta, \tag{3}$$

where θ is the phase of the qubit state. The probability amplitude of $|0\rangle$ and $|1\rangle$ corresponds to the real and imaginary parts of Eq. (3), respectively.

The qubit neuron model is constructed from a one-qubit rotation quantum gate and two-qubit controlled NOT (CNOT) quantum gate, as described below

$$u = \sum_{l}^{L} f(\theta_l) f(y_l) - f(\lambda), \tag{4}$$

$$y = \frac{\pi}{2} g(\delta) - \arg(u), \tag{5}$$

$$O = f(y), \tag{6}$$

where $g(x) = 1/[1+\exp(-x)]$ and arg represents the phase extracted from a complex number. Here, O is the output of the qubit neuron model which receives inputs from L other neurons. The connection phase parameter θ and threshold λ correspond to the rotation gate, and the reversal parameter δ corresponds to the CNOT gate.

3.2 *Computer-Generated Hologram Compression with Quantum-Inspired Neural Network*

The qubit-based QINN has been proved to be effective in CGH compression.[1] It is constructed by replacing neurons with the qubit neurons in a conventional neural network, and targets and inputs are expected to be equal (e.g., L).

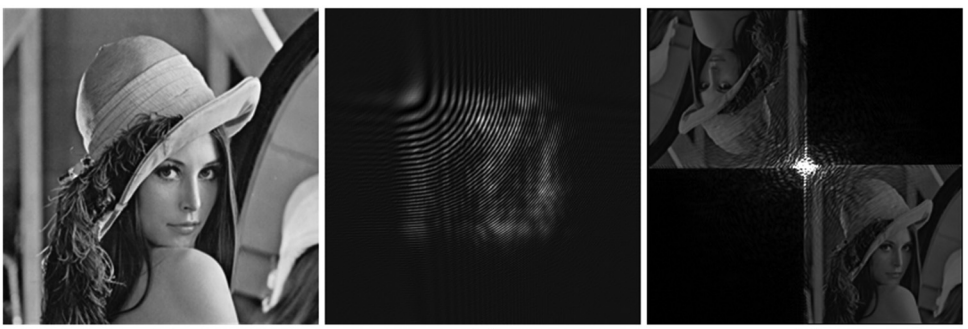

(a) (b) (c)

Fig. 2 CGH of a gray-scale Lena image and the corresponding reconstructed image. (a) Original Lena image (128×128 pixels), (b) CGH (256×256 pixels), and (c) reconstructed image (256×256 pixels).

With a narrow hidden layer (e.g., K, $K < L$), the hidden layer outputs the compressed image data. Thus, the input and hidden layers are regarded as an encoder, while the hidden and output layers are regarded as a decoder.

During compression, a CGH image is preprocessed by a linearly normalization from the range of [0, 255] into the range of [0,1]. Then the normalized CGH (e.g., $X \times Y$ pixels) is divided into nonoverlapping pixel blocks [e.g., $x \times y$ pixels, $N = (X \times Y)/(x \times y)$ blocks in total] and is converted to vectors (e.g., $L \times 1$, $L = x \times y$) as training samples. All vectors are fed into the network and trained with an error backpropagation learning algorithm. Different CRs can be obtained by varying the numbers of hidden neurons (K). The output of n'th neuron in the last layer represents the observed probability of $|1\rangle$, which is defined as

$$\text{output}_n = |\text{Im}(O_n)|^2. \tag{7}$$

4 Computer-Generated Hologram Quality Improved with Parallel Structure Network and Residual Learning

4.1 *Computer-Generated Hologram Quality Improved with Parallel Structure Network*

When compressing an image with networks, compression performance often decreases with the decrement of the hidden layer neurons; it is because the number of neurons in the hidden layer directly affects the fitting ability of the network. To improve the fitting ability, one method involves increasing the number of network layers, but more network layers encounter many disadvantages including the increasing of convergence time. Apart from this method, we have tried choosing a parallel network structure,[12] as shown in Fig. 3.

Several sub-QINNs (e.g., N. $Net_1, \ldots, Net_i, \ldots, Net_N$) are used to construct the parallel network, where each of the sub-QINN has L input units, K ($K < L$) hidden units, and L output units. During compression, the pixel blocks in a CGH are partitioned into several subsets (e.g., N) according to complexity, and each subset is trained by a sub-QINN, respectively. Because pixel blocks with similar features can be trained by the same subnetwork, the parallel structure QINN can better fit the CGH.

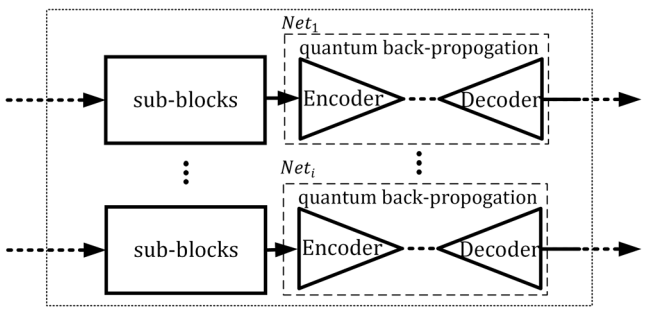

Fig. 3 Parallel QINN structure for CGH quality improvement.

4.2 *Computer-Generated Hologram Quality Improved with Residual Learning*

CGH compression using the QINN is a lossy compression method and always brings heavy artifacts and bad subjective quality, especially at high compression rate. The information lost from the compressed CGH can be regarded as the noise introduced during compression. We can define the compression process as

$$y = F(x) = x + n, \tag{8}$$

where x is an original CGH, y is the compressed CGH, F indicates the compression process, and n is the noise added during compression. The compressed CGH can be improved when n can be well predicted. To this end, a deep feed-forward CNN to improve the quality of the compressed CGH is added to our framework, as shown in Fig. 1. The residual learning formulation is adopted to train a residual mapping function R

$$R(y) \approx n. \tag{9}$$

The residual CGH can be predicted from the CNN, and the improved CGH can be obtained from the following equation:

$$\overline{x} = y - R(y). \tag{10}$$

The averaged mean squared error between the desired residual CGHs and the estimated CGHs due to noisy input is described by the network loss function, which is given as

$$l(\Theta) = \frac{1}{2N}\sum_{i=1}^{N} \|R(y_i, \Theta) - (y_i - x_i)\|^2, \tag{11}$$

where Θ is the trainable parameter in the CNN and N is the number of CGH training pairs.

The denoising convolutional neural network (DnCNN)[13] has been used in our method, as shown in Fig. 4. The output from each layer in the DnCNN has the same width and height to confirm the same size of the network inputs and outputs. The network depth is set to 17. The first layer uses a convolution layer (Conv) with 64 3×3 filters and rectified linear units (ReLUs). Layers 2 to 16 each contains a Conv with 64 $3 \times 3 \times 64$ filters and batch normalization, where ReLUs are used in each layer. The final layer uses a single Conv with one $3 \times 3 \times 64$ filter.

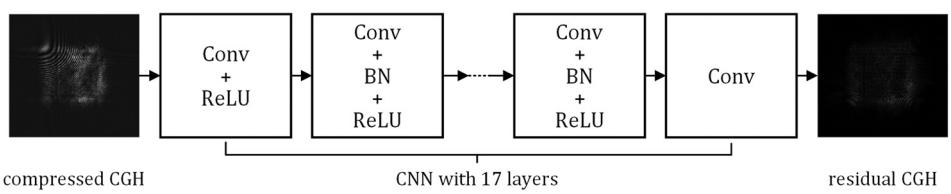

Fig. 4 Deep convolutional network structure for CGH quality improvement.

5 Experimental Results and Analysis

5.1 *Quality Evaluation of Reconstructed Image*

In our experiments, the CR and peak signal-to-noise ratio (PSNR) are used to evaluate the quality of reconstructed CGH

$$\mathrm{CR} = \frac{S_c}{S_o} = \frac{K}{L}, \tag{12}$$

$$\mathrm{MSE} = \frac{1}{X \times Y} \sum_{x=1}^{X} \sum_{y=1}^{Y} |f(x,y) - \overline{f}(x,y)|^2, \tag{13}$$

$$\mathrm{PSNR} = 10 \log_{10} \frac{x_{\mathrm{peak}}^2}{\mathrm{MSE}}, \tag{14}$$

where $f(x,y)$ and $\overline{f}(x,y)$ are the reconstructed image function of the original CGH ($X \times Y$ pixels) and the compressed CGH, respectively. Here, x_{peak} is the peak-to-peak value of the CGH and MSE is the mean squared error.

5.2 *Optimized Initial Weight*

To quickly transmit the holographic data and improve the reconstructed image quality of the compressed CGH, we utilize the pretraining strategy to initialize the QINN. First, the training set of CGHs generated from different objects are utilized to pretrain the QINN, a network model with generalization ability is obtained and regarded as an optimized initial weight after pretraining stops. Then the QINN is initialized with the optimized initial weight and is further trained with the pixel blocks divided from the CGH to be compressed. Once training completes, the QINN will be ready for CGH compression where half of the QINN acts as an encoder and the other half as a decoder. Since the optimized initial weight is very close to the optimized solution and is maintained the same throughout the compression process, the compression process time can be drastically reduced (i.e., the strategy of pretrain with Gradient Descent, Pretrain+GD).

We randomly chose 20 images from the LIVE1 dataset,[14] cropped and resized the images, and generated corresponding Fresnel off-axis CGHs (256×256) as the training set of CGHs. Each CGH was divided into 8×8 nonoverlapping blocks and set as the input and target of the network for pretraining the initial weights. The number of neurons in the input and output layers was 64, and the number of neurons K in the hidden layer was varied to obtain different CRs (e.g., $K = 32, 16, 8, 4$). The QINN network weight after 2000 training epochs was chosen as the optimized initial weight.

An untrained CGH generated from a gray-scale Lena image (from the Classic5 dataset) was compressed using the QINN. We set a tolerance MSE (E_{max}), as shown in Table 2. Once the network *MSE* was less than E_{max}, we ended the training process and considered it to have converged. The best learning rate (lr) for our strategy of Pretrain+GD is described in Table 2.

We also compared our strategy of Pretrain+GD with the strategy described in Refs. 1 and 15. In Ref. 1, the CGH to be compressed is directly regarded as the training set as well as the testing set and fed into the qubit-based QINN, which causes the network weight to be trained from scratch for each CGH. In addition, the QINN is randomly initialized without effective strategy (i.e., the strategy of Random Initialization with Gradient Descent, Random+GD). The best learning rate (lr) for the strategy of Random+GD is also described in Table 2. In Ref. 15, the compression network is Only Pretrained with a large number of images, and the CGH to be compressed is not included in the training set and without further training. The network image compression system has the ability to compress an untrained image but with lower compression performance than using the trained image (i.e., the strategy of Only Pretrain).

The number of iterations and the reconstructed image PSNR of the CGH using three different compression strategies for different K values in the hidden layer are shown in Table 3. We perform five learning trials for the three strategies in order to obtain stable results. The best result for each K is highlighted in bold. One can see that our Pre-train + GD strategy can reduce the number of required compression iterations compared with the Random + GD strategy and it yields better reconstructed image quality of the CGH compared with the Only Pretrain strategy. For example, in the

Table 2 E_{max} and the best learning rate.

K	CR	E_{max}	Best lr (Random + GD)	Best lr (Pre-train + GD)
32	0.5000	0.000380	0.25	0.20
16	0.2500	0.001272	0.3	0.20
8	0.1250	0.002062	0.2	0.10
4	0.0625	0.002630	0.25	0.06

Table 3 Number of iterations and PSNR of the reconstructed CGHs after compression.

	Random + GD		Only Pretrain		Pre-train + GD	
K	Iterations (epoch)	PSNR (dB)	Iterations (epoch)	PSNR (dB)	Iterations (epoch)	PSNR (dB)
32	4149 ± 810	25.31 ± 0.19	—	25.35 ± 0.13	$\mathbf{26 \pm 5}$	$\mathbf{26.02 \pm 0.05}$
16	4118 ± 1164	20.51 ± 0.66	—	20.55 ± 0.13	$\mathbf{33 \pm 14}$	$\mathbf{21.06 \pm 0.07}$
8	4391 ± 1018	18.68 ± 0.60	—	18.51 ± 0.06	$\mathbf{17 \pm 6}$	$\mathbf{18.77 \pm 0.10}$
4	3924 ± 1594	$\mathbf{17.90 \pm 0.17}$	—	17.14 ± 0.13	$\mathbf{25 \pm 54}$	17.32 ± 0.26

Note: The best result for each K is highlighted in bold, as described in paper.

case of $K = 8$, our Pre-train + GD strategy requires 17 average epochs to converge, while the Random + GD strategy requires 4391 average epochs. It is reasonable that the training phase of the Random + GD strategy is included in the compression process, which is nonreusable and time-consuming. Owing to having no further training process for a specific CGH, the Only Pretrain strategy does not require any iterations for further training. For the Pre-train + GD, Only Pretrain, and Random + GD strategies, the reconstructed PSNR values of the CGH are 18.77, 18.51, and 18.68 dB, respectively. The Pre-train + GD strategy outperforms the Only Pretrain and Random + GD strategies. The generalized network model in the Only Pretrain strategy can compress the untrained CGH, but its PSNR value is lower than the trained CGH in Pre-train + GD. In the case of $K = 4$, we find that the Random + GD strategy can reconstruct a CGH with higher image quality. It is because the pretrained model for initialization cannot provide very precise guess for the network when the compression network has less parameters for learning. The Random + GD strategy which is trained with more iterations can get higher PSNR.

Figure 5 shows the PSNR of reconstructed CGH as a function of the number of training iterations. One can see that our Pre-train + GD strategy gets better performance from the beginning of the learning stage with respect to different CRs. The optimized initial weight offers a better initial state, which is close to the optimized solution. It also indicates that the fitting ability of the QINN decreases as the CR increases.

5.3 *Computer-Generated Hologram Compression with Parallel Quantum-Inspired Neural Network Structure*

In experiments, two QINNs with the same structure were combined to establish a QINN with parallel structure. About 20 CGHs from the LIVE1 dataset were used again to generate the CGHs. A CGH from a gray-scale Lena image [Fig. 2(a)] was used to test the performance of the parallel structure QINN.

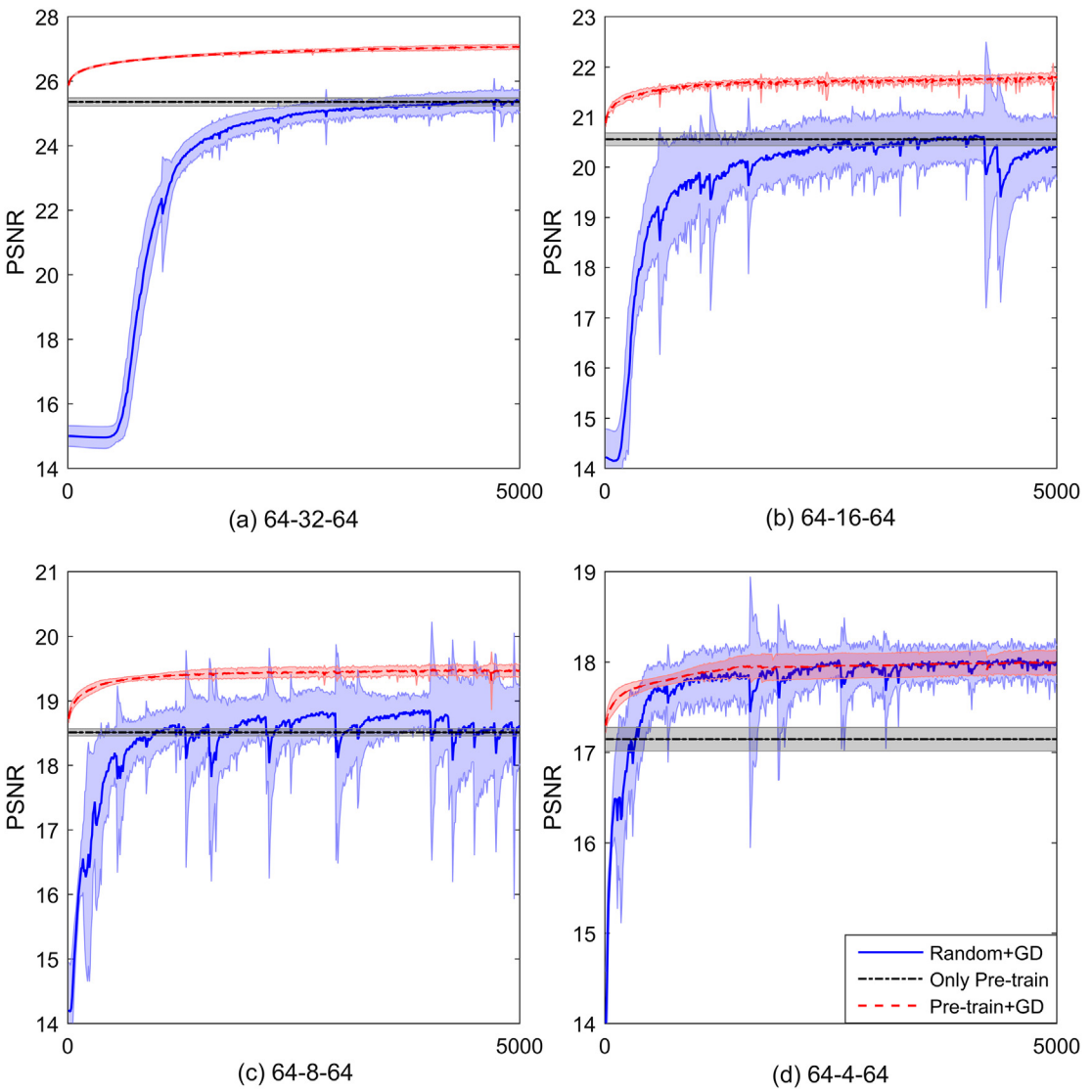

Fig. 5 Reconstructed images PSNRs of CGHs change with the increment of training iterations. Horizontal coordinate represents the iteration echos. Here, "64-32-64" stands for the stacked layer width (input layer width—hidden layer width—output layer width, respectively).

Table 4 The average PSNR of CGH reconstructed using single QINN structure and parallel QINN structure.

	Only Pretrain		Pre-train + GD (with 10 epochs)	
K	Single (dB)	Parallel (dB)	Single (dB)	Parallel (dB)
32	25.35 ± 0.13	$\mathbf{25.81 \pm 0.12}$	25.87 ± 0.04	$\mathbf{26.04 \pm 0.06}$
16	20.55 ± 0.13	$\mathbf{20.71 \pm 0.14}$	20.84 ± 0.10	$\mathbf{20.91 \pm 0.09}$
8	18.51 ± 0.06	$\mathbf{18.65 \pm 0.10}$	18.72 ± 0.07	$\mathbf{18.81 \pm 0.09}$
4	17.14 ± 0.13	$\mathbf{17.39 \pm 0.17}$	17.30 ± 0.08	$\mathbf{17.50 \pm 0.15}$

Note: The best result for each K is highlighted in bold, as described in paper.

During the training stage of the parallel QINN, the pixel blocks from the CGH were first applied to train a coarse model (after 1000 training epochs) in a single QINN, and then the PSNR for the coarse model was used to classify the pixel blocks of each CGH into two parts. After the coarse classification had completed, a category table for block classification was voted by the classification results of each CGH. According to the category table, the CGH pixel blocks were classified into two subsets, and each subnetwork in the parallel QINN structure was initialized using the coarse model and further trained (1000 training epochs) by the corresponding subsets, respectively.

For the purposes of comparison, the single QINN structure was trained directly with 2000 epochs, and all networks were trained with a fixed learning rate of 0.1. We applied two Only Pretrain and Pre-train + GD compression strategies to the parallel QINN structure. In the Pre-train + GD strategy, the number of iterations used for further training was set to 10 epochs. In the Only Pretrain strategy, no further training was required when compressing a CGH.

The average PSNRs of CGH reconstructed using a single QINN and the parallel QINN structure are listed in Table 4. When the Only Pretrain compression strategy is applied in the parallel structure QINN, we can see that the parallel structure QINN obtains better PSNR for different CRs, improves the generalizability of the model, and provides a better optimized initial weight. When the Pre-train + GD compression strategy is applied in the parallel QINN structure, the parallel QINN structure yields better PSNR of the reconstructed CGH due to the better initial weight.

5.4 *Computer-Generated Hologram Quality Improvement with Residual Learning*

To obtain a deep feed-forward CNN model for improving the quality of the compressed CGH, the DnCNN network was used and fine-tuned using the CGH generated from the BSD68 dataset (68 natural images).[16] The CGH blocks after compression with the Pre-train + GD strategy were set as inputs, and the residual blocks between the original and compressed CGHs were set as labels. The input patch size of the improved CNN was 40×40.

CGHs generated from the classic5 (5 images), Set5 (5 images), and Set12 (12 images) datasets were used for testing. Stochastic gradient descent (SGD) was used with weight decay of 0.0001, a momentum of 0.9, and a batch size of 64 to train the model based on the DnCNN. The learning rate was decayed from 0.01 to 0.001 over the 40 epochs. The MatConvNet package was used to train the proposed improvement models. All the experiments were carried out in MATLAB (R2015b) running on a PC with an Intel(R) Xeon(R) E5-2620 v2 2.1 GHz CPU and an NVIDIA K2000 GPU.

Table 5 Average PSNRs of compressed CGH of the reconstructed image with or without the improved CNN.

K	Classic5	Set5	Set12
32	26.54/**36.09**	26.56/**35.17**	26.46/**35.98**
16	21.72/**30.12**	21.62/**29.25**	21.73/**29.88**
8	19.33/**27.92**	19.37/**26.67**	19.45/**27.52**
4	17.95/**23.89**	18.01/**23.04**	18.02/**23.66**

Note: The best result for each K is highlighted in bold, as described in paper.

The average PSNRs of the reconstructed image from the compressed CGH with or without the improved CNN are listed in Table 5. One can see that the improved CNN can effectively improve the quality of the reconstructed image from the compressed CGH. In the case of $K = 32$, the reconstructed CGH obtains a notable PSNR improvement of about 9.55, 8.61, and 9.52 dB with the Classic5, Set5, and Set12 datasets, respectively. It should be noted that the average processing time of each CGH with the improved CNN is <0.38 s. The PSNR of the reconstructed Lena image from the compressed CGH with/without the improved CNN is shown in Fig. 6.

Visual comparisons of the reconstructed images from the compressed CGH are shown in Fig. 7. Figure 7(d) shows the image reconstruction of CGH without compression, Fig. 7(e) shows the image reconstructed from the compressed CGH, and Fig. 7(f) shows the image reconstructed of compressed and improved CGH. One can see that the improved CNN can

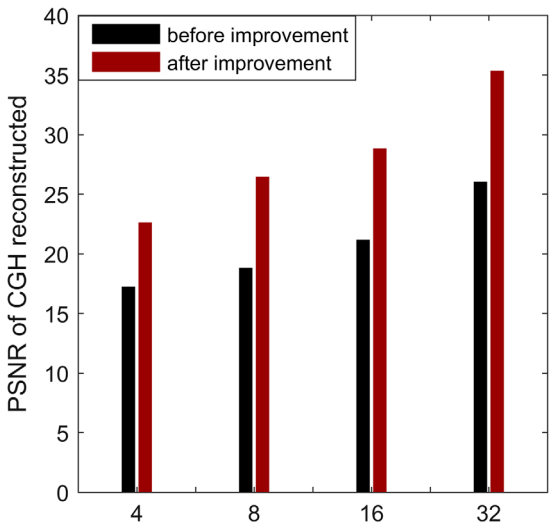

Fig. 6 The average PSNR of the reconstructed Lena image from the compressed CGH with/without the improved CNN. Horizontal coordinate stands for the hidden layer width.

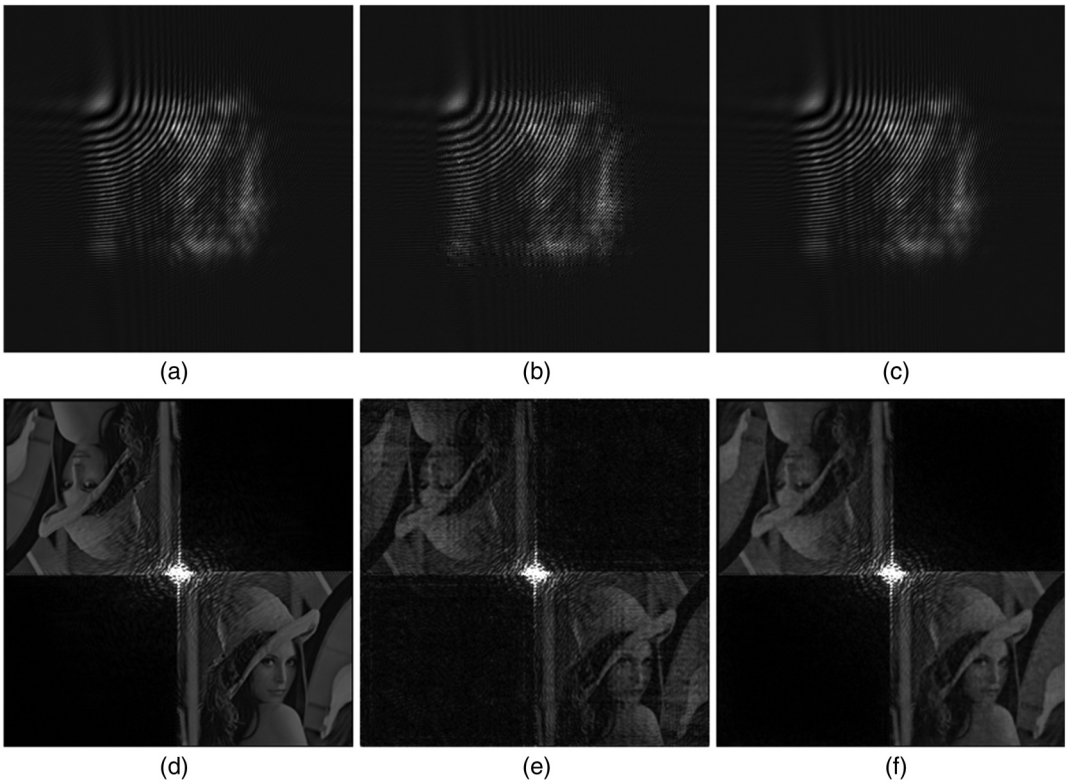

Fig. 7 Comparison of CGHs and their reconstructed images with $K = 32$. (a) CGH without compression, (b) CGH after compression, (c) CGH after compression and improvement, (d) reconstructed image of (a), (e) reconstructed image of (b), and (f) reconstructed image of (c).

eliminate the distortion and reduce saliency noise in the smooth region, and the fine details of the reconstructed images are recovered to yield better visual results. The experimental results indicate the feasibility of deploying our method for CGH compression.

6 Conclusion

We have proposed an optimized initial weight scheme for QINN applied to CGH compression, which can improve the quality of the reconstructed image from the compressed CGH. The results show that the optimized initial weight for the QINN obtained by pretraining yielded a better initial network state, which is close to the optimized solution and reduces the number of network compression iterations. Also, the parallel structure can improve the adaptive ability of QINN, and the deep CNN model with residual learning can effectively reduce compression noise and improve the reconstructed image quality of the compressed CGH. The experimental results show that the scheme is effective compared to other strategies. In the future, GPU version QINN will be applied to practice and integrated with the followed residual learning network.

Acknowledgments

The authors would like to thank the Spatial Image Processing Laboratory for their support. This work was supported by the National Science Foundation of China (Grant No. 61271310).

References

1. M. Liu, G. Yang, and H. Xie, "Method of computer-generated hologram compression and transmission using quantum back-propagation neural network," *Opt. Eng.* **56**(2), 023104 (2017).
2. G. Yang and E. Shimizu, "Information compressed and transmitted and reconstructed system of CGH with LOCO-I image processing and Fraunhofer transforming technique," *IEEJ Trans. Electron. Inf. Syst.* **120**(11), 1520–1527 (2000).
3. Y. Sun, G. Yang, and H. Xie, "Computer-generated hologram fast transmission using compressive sensing," in *OSA Technical Digest (online), Imaging and Applied Optics 2016*, p. JW4A.34 (2016).
4. G. Yang, C. Zhang, and H. Xie, "Information compression of computer-generated hologram using BP neural network," in *OSA Technical Digest (CD), Biomedical Optics and 3-D Imaging*, p. JMA2 (2010).
5. A. L. Hou et al., "Computer-generated hologram compression research based on bp neural network in wavelet domain," *Adv. Mater. Res.* **971–973**, 1884–1887 (2014).
6. A. W. Lohmann and D. Paris, "Binary Fraunhofer holograms, generated by computer," *Appl. Opt.* **6**(10), 1739–1748 (1967).
7. N. Kouda, N. Matsui, and H. Nishimura, "Learning performance of neuron model based on quantum superposition," in *Proc. 9th IEEE Int. Workshop on Rob. and Hum. Interactive Commun., RO-MAN 2000*, pp. 112–117 (2000).
8. N. Kouda, N. Matsui, and H. Nishimura, "Image compression by layered quantum neural networks," *Neural Process. Lett.* **16**(1), 67–80 (2002).
9. N. Kouda et al., "Qubit neural network and its learning efficiency," *Neural Comput. Appl.* **14**(2), 114–121 (2005).
10. S. Ganjefar et al., "Training qubit neural network with hybrid genetic algorithm and gradient descent for indirect adaptive controller design," *Eng. Appl. Artif. Intell.* **65**, 346–360 (2017).
11. E. N. Leith and J. Upatnieks, "Reconstructed wavefronts and communication theory," *J. Opt. Soc. Am.* **52**(10), 1123–1130 (1962).
12. S. Carrato and S. Marsi, "Parallel structure based on neural networks for image compression," *Electron. Lett.* **28**(12), 1152–1153 (1992).
13. K. Zhang et al., "Beyond a Gaussian denoiser: residual learning of deep CNN for image denoising," *IEEE Trans. Image Process.* **26**(7), 3142–3155 (2017).
14. H. R. Sheikh et al., "LIVE image quality assessment database release 2" (2005).

15. O. N. Al-allaf, "Improving the performance of backpropagation neural network algorithm for image compression/decompression system," *J. Comput. Sci.* **6**(11), 1347–1354 (2010).
16. D. Martin et al., "A database of human segmented natural images and its application to evaluating segmentation algorithms and measuring ecological statistics," in *Proc. Eighth IEEE Int. Conf. Comput. Vision, ICCV 2001*, pp. 416–423 (2001).

Shenhua Hou received his BEng degree from Electronic Information School, Wuhan University, China, in 2015 and his MEng degree from School of Electronics Engineering and Computer Science, Peking University, China, in 2018. His research interests include image processing and digital holography.

Guanglin Yang has been an associate professor at Peking University since 2002. He became a lecturer at Beijing University of Aeronautics and Astronautics of China in 1994. He received his DEng degree from Osaka City University of Japan in 2001 and his MEng degree from Huazhong University of Science and Technology of China in 1993. His research interests mainly include optical imaging, digital holography, and image processing. He is a member of IEEE and a senior member of OSA.

Haiyan Xie is a patent attorney at China Science Patent Trademark Agents Ltd. She received her MS and PhD degrees from Osaka City University of Japan in 2002 and 2005, respectively. She received her BEng and MEng degrees from Zhejiang University of China in 1990 and 1992, respectively. She became a lecturer at Beijing University of Aeronautics and Astronautics of China in 1995. Her research interests mainly include thin film optics and semiconductor material.